Numerical Simulation Analysis of Non-Contact Mechanical Seal Performance based on Dynamic Grid Technology

Chunyuan Li

Abstract—**By applying the dynamic mesh technology of FLUENT software to the numerical simulation of internal flow field in mechanical seal clearance, the problem of unpredictable liquid film thickness in the simulation process can be solved, and a more actual internal flow field characteristic can be obtained. The flow of sealing fluid between the end faces of moving and stationary rings is affected by the superposition of differential pressure flow and shear flow. The clearance seal performance is studied by using computational fluid dynamics (CFD), and the influence of pressure difference, axial seal length and rotor speed on the sealing performance is analyzed. The experimental results show that the leakage of the seal gap increases with the increase of the pressure difference, changes linearly with the rotation speed, and is inversely proportional to the rotation speed. The larger the speed, the smaller the leakage. The longer the axial length of the seal, the smaller the leakage of the seal clearance. The numerical simulation value obtained by the dynamic grid method is close to the experimental value under three different speeds. It is feasible to apply the dynamic grid technology to the simulation of the internal flow field of mechanical seals, and good results can be achieved.**

Index Terms—**Dynamic mesh technology; Non-contact machinery; Sealing performance; Numerical simulation**

I. Introduction

In the operation process of mechanical seal, the thickness of liquid film on the end face is directly related to the seal structure, medium pressure, end face modeling, internal flow field characteristics and rotation speed. Therefore, the liquid film thickness is unpredictable in the numerical simulation of the internal flow field between the end faces, which brings difficulties to the simulation calculation [1]. The main and auxiliary seals are non-contact seals, including non-contact gas film seal and non-contact liquid film seal. The main seal is used to seal high-temperature medium, and the auxiliary seal plays a role of safety sealing, so as to realize zero leakage of high-temperature medium [2]. By calculating the temperature field of the high temperature pump, it is known that there is a certain temperature difference between the inner and outer diameters of the dynamic and static rings; in fact, the outer temperature is relatively higher. Therefore, the viscosity of the fluid film is not a constant value, but a variable that will change with the temperature. During the sealing operation, the viscosity will change with the temperature change, which will affect the performance of the fluid film, such as the opening of the gas film. The lifting force and stiffness may change the film thickness during stable operation [3]. The sealing form is single-sided bellows seal with cold water flushing device. When using it, the medium leakage occurred only three months ago. Therefore, it needs to be repaired frequently, which not only wastes a lot of manpower and financial resources, but also requires a high oil temperature over 350 ℃, which may easily cause fire accidents. Therefore, the improvement of non-contact mechanical seal is imperative [4].

The dynamic grid can be used to simulate the time-dependent change of flow field shape. The motion form of flow field boundary can be pre-defined motion, that is, the boundary motion law is known before calculation, and its velocity or angular velocity is specified in advance; or it can be undefined motion, that is, the motion law of boundary cannot be predicted but must be determined by the calculation results of the previous step [5]. The mesh updating process is automatically completed by fluent according to the boundary changes in each iteration step. In the numerical simulation of the internal flow field of mechanical seals, the dynamic mesh technique with undefined boundary motion can be used [6]. The relationship between the boundary motion and the parameters in the internal flow field is defined by the user, and the program is dynamically connected to the fluent solver, so as to realize the function of changing the mesh shape and boundary motion characteristics in the iterative solution process, which makes the mechanical model closer to the reality.

II. Dynamic Grid Technology

The moving mesh technique is applied to the calculation of moving boundary problems. The motion of the boundary can be realized by specifying the linear velocity or angular velocity in advance, and the motion can be realized by iterating the calculation results of the previous step [7]. The initial state of the grid must be defined before calculation. After the boundary motion or deformation occurs, the grid update of the watershed follows the grid update method selected by the user. The moving grid model solves the unsteady problem, which occupies a lot of hardware resources.

Manuscript received April 21, 2022; revised November 25, 2022.

C. Y. Li is an Associate professor of the Institute of Mathematics and Statistics of Baicheng Normal University, Baicheng, TX 137000 China. (corresponding author e-mail: chunyuanli0410@163.com).

For an arbitrary control volume, the integral conservation equation of generalized scalar Φ is as follows:

$$\frac{d}{dt}\int_v \rho\Phi dV + \int_{\partial v} \rho\Phi\left(u - u_g\right)dA = \int_{\partial v} \Gamma\nabla\Phi dA + \int_v S_\Phi dV \qquad (1)$$

Where ρ is the density of liquid; u is the velocity vector; u_g is the moving speed of the grid; Γ is the diffusion coefficient; S_Φ is the source term; ΔV is the boundary of control volume V.

Figure 1(a) shows the cross-sectional view of the sealing chamber. The left side is the high-temperature oil inlet. The pressure inlet is set to 0.45 MPa. The inner wall and moving ring surface are set as the rotating walls, and the rotating speed is set to310.86 rad/s. The outer wall and stationary ring surface are set as static walls. Figure 1(b) shows the grid model diagram of high temperature oil in the seal chamber, which is divided into triangular grids with the grid number of 286014, with the inclination rate not exceeding 0.8. The grid is in good condition. The flow state of high-temperature oil can be calculated with Ta standard number.

$$Ta = \frac{2\eta^2 d^4}{1-\eta^2}\left(\frac{\Omega}{\upsilon}\right)^2 = 1.12\times10^7 > 1000Ta_c = 2.279\times10^6 \qquad (2)$$

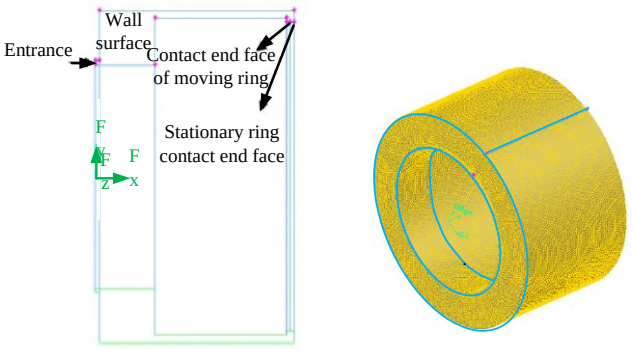

(a) Section (b) Grid graph

Fig. 1. Schematic diagram of shaft sleeve clearance model establishment

The dynamic layer updating method is used to update the dynamic mesh, and the constant scale method is used to segment the mesh layer. The split factor is set to 0.4 and Shrinkage factor is set to 0.04. The dynamic mesh characteristic parameters of bearing clearance are analyzed by using the block area mesh generation method of dynamic mesh generation technology and the directivity gain control method, and the finite universe of bearing clearance is obtained. Combined with the method of fuzzy subsequence fusion scheduling, the E-Learning learning model of bearing clearance is constructed by using embedded program scheduling. By mining frequent item sets, the reliable behavior mode of the sealing surface is obtained, and the associated nodes of the flow seal are used for regional scheduling in blocks. The autocorrelation feature distribution set of sealing feature is represented in the form of triple. Therefore, the method of grid fusion by blocks is adopted to improve the ability of grid segmentation of shaft sleeve clearance.

III. Numerical Simulation Of Non-Contact Mechanical Seal Performance

This paper studies the non-contact internal flow mechanical seal performance of clearance liquid film. The internal flow seal refers to the mechanical seal in which the fluid leakage direction between the seal faces is opposite to the centrifugal force direction. On the contrary, the mechanical seal with the same leakage direction and centrifugal force direction between seal faces is called external flow mechanical seal [8]. Since the centrifugal force can not only prevent the leakage of fluid, but also prevent the solid particles from entering the sealing surface, the leakage of the internal flow seal is smaller than that of the external flow seal (Figure 2(a); Figure 2(b)). Generally, the internal flow mechanical seal works well under high pressure, and the maximum pressure of the external flow mechanical seal is 1 ~ 2 MPa.

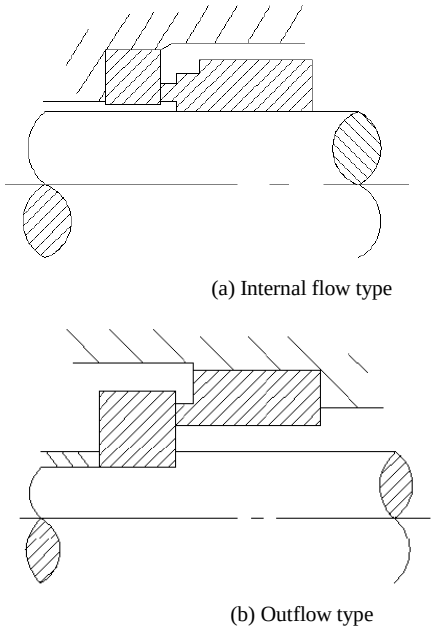

(a) Internal flow type

(b) Outflow type

Fig. 2. Liquid film in the end clearance of non-contact internal flow mechanical seal

After selecting the model, the three-dimensional numerical simulation of the pressure field of its end face is carried out by FLUENT software. For the contact mechanical seal, the seal faces should be kept parallel as far as possible, because the parallel face model is the most ideal seal model, which can effectively reduce wear, reduce leakage, prolong seal life and improve sealing performance [9].

Before modeling and meshing, it is necessary to determine the flow state of the liquid film in the end gap. Due to the existence of the pressure difference between the inner and outer diameters in the seal ring gap, the sealing fluid flows from the high-pressure side to the low-pressure side. In addition, the rotation of the moving ring causes shear effect between the moving ring surface and the fluid. Therefore, the flow of the sealing fluid between the end faces of the dynamic and static rings is affected by the superposition of the differential pressure flow and the shear flow [10].

In order to determine the flow state, it is necessary to consider the coupling effect of the two flows, that is, the flow state is determined by two Reynolds numbers R_{ec} and R_{ep}. When judging the flow in the seal gap, the change of flow

factor α is used to represent the change process from laminar flow to turbulent flow. Figure 3 shows the change of flow factor α.

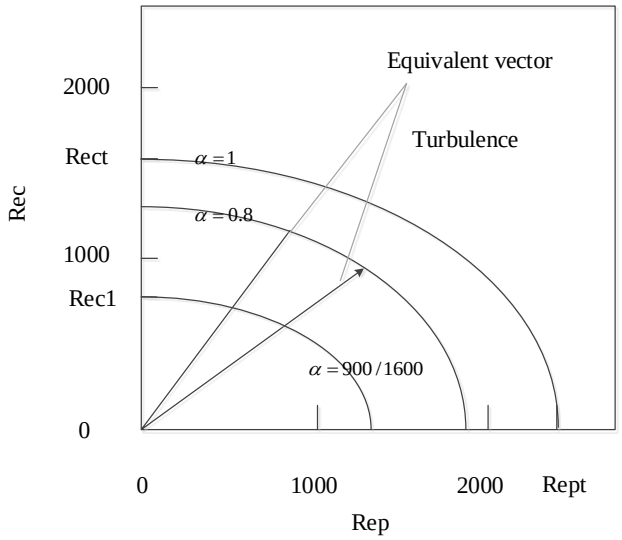

Fig. 3. Variation of flow factor α

When $\alpha>1$, the flow in the seal face clearance is in turbulent state; When $\alpha<(9/16)$, the flow in the seal face clearance is in laminar flow state.

$$\alpha=\sqrt{\left(\frac{R_{ec}}{1600}\right)^2+\left(\frac{R_{ep}}{900}\right)^2} \tag{3}$$

Where R_{ec} is the shear flow Reynolds number and R_{ep} is the radial flow Reynolds number, which can be expressed as follows:

$$R_{ec}=\frac{\rho U h_0}{\mu} \tag{4}$$

$$R_{ep}=\frac{\rho V_r h_0}{\mu} \tag{5}$$

Where U is the linear velocity of the end face of moving ring, m/s, V_r is the radial velocity of the sealing fluid, m/s, h_0 is the thickness of the fluid film, m.

According to the end clearance of mechanical seal, the physical model as shown in the figure is established, where $z=0$ represents the end face of moving ring and $z=h(x,y)$ represents the end face of static ring.

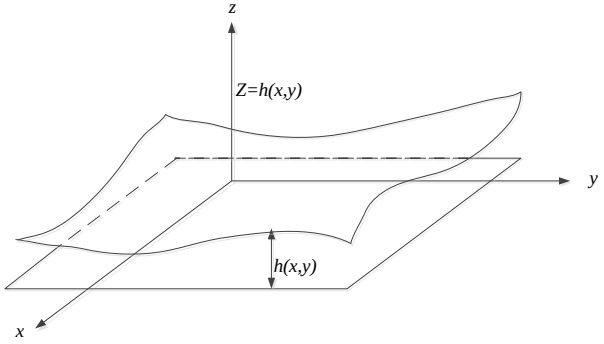

Fig. 4. Geometric model of liquid film

Generally, the sealing performance is measured by taking the leakage rate as a variable. For the fluid lubrication state, the mass leakage derived from the radial plane gap pressure difference flow is as follows:

$$G=\frac{\frac{1}{n}\pi h^3\left(p_2^n-p_1^n\right)}{6\mu v\cdot\ln\frac{R_2}{R_1}\cdot p_2^{n-1}} \tag{6}$$

Where v is the specific volume.

The sealing device described in this paper is a non-contact mechanical seal, for which the leakage of medium is inevitable [11]. Leakage is an important parameter determining the performance of seal. Among the factors that affect the leakage, the size of the end seal clearance is particularly important. The governing equation of leakage of parallel face seal is as follows:

$$W=\frac{1}{n}\pi h^3\frac{R_2}{R_1}\left(p_2^n-p_1^n\right) \tag{7}$$

According to the above formula, the leakage is related to the seal clearance h. Take $h=1\text{n}10\mu m$, calculate and analyze the size of the leakage, and draw a graph to observe the relationship between the leakage and the seal clearance.

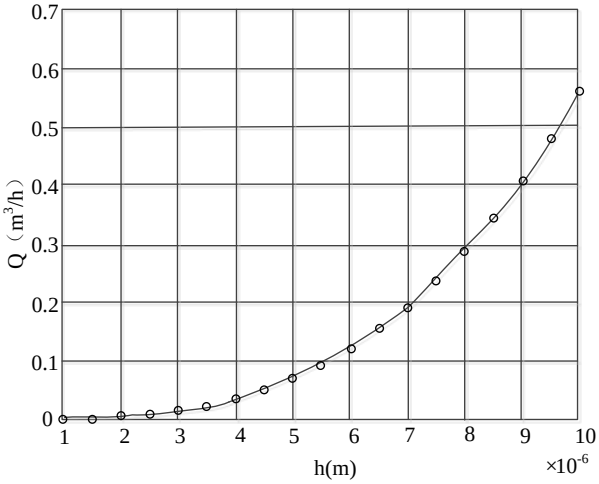

Fig. 5. Change of leakage Q with seal clearance h

It can be seen from Figure 5 that the leakage rate increases with the increase of seal clearance in an exponential manner.

According to the forming theory of traditional mechanical seal fluid film and the characteristics of FLUENT software, continuity equation and N-S equation are selected as control equations:

$$\frac{\partial u_i}{\partial x_i}=0 \tag{8}$$

$$\frac{\partial u_i}{\partial t}+u_j\frac{\partial u_i}{\partial x_i}=F_i-\frac{1}{\rho}\frac{\partial p}{\partial x_i}+\nu\frac{\partial^2 u_i}{\partial x_j\partial x_j} \tag{9}$$

Where, u_i is velocity, p is positive pressure, F_i is volume force, ρ is fluid density, i, j are free indexes, of which the value is $1,2,3$.

The gap sealing performance is studied by using

computational fluid dynamics (CFD). The fluid flow in the seal gap satisfies the following equation:

A. Mass conservation equation:

$$\frac{\partial \rho}{\partial t}+\nabla(\rho u)=0 \tag{10}$$

$\nabla=\frac{\partial}{\partial x}+\frac{\partial}{\partial y}+\frac{\partial}{\partial z}$, ρ is the density of the fluid and u is the velocity of the fluid.

B. Momentum conservation equation:

$$\rho\frac{\partial u}{\partial t}+\rho(u\cdot\nabla)u=\nabla\cdot\sigma+F \tag{11}$$

F is the mass force per unit volume and σ is the stress per unit volume.

C. Energy conservation equation:

$$\frac{\partial(\rho T)}{\partial t}+div(\rho uT)=div\left(\frac{k}{c_p}gradT\right)+s_T \tag{12}$$

Where T the temperature of the medium is, c_p is the specific heat capacity of the medium, s_T is the viscous dissipation, and k is the heat transfer coefficient. In the calculation process, it is assumed that the sealing surface is absolutely smooth, and the influence of seal surface roughness can be ignored [12-14]. Due to the viscosity of the liquid, there is internal friction between the liquids, and there is a hydraulic pressure difference between the end faces of the seal. When the pressure difference of the seal end face is less than the internal friction force between the fluids, the liquid in the seal gap will not flow, thus playing a role in sealing [15-17].

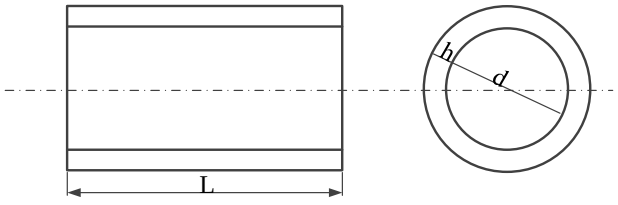

Fig. 6. Seal of mouth ring

For the ring seal as shown in Figure 6, assuming that the high-pressure side pressure is P1, the low-pressure side pressure is P2, the seal gap size is h, the sealing length is L, the medium flow rate is V, the medium viscosity is μ, and the axial direction is X direction, then the internal friction force between the liquids can be calculated as follow:

$$\varepsilon_r=-\mu Lh\frac{dV}{dx} \tag{13}$$

If the pressure distribution is linear, the thrust formed by the oil film is:

$$F=\int_{r_1}^{r_2}2\pi r dr\,\mathrm{Pr} \tag{14}$$

r_1 is the radius of the inner cylindrical surface of the seal and r_2 is the radius of the outer cylindrical surface of the seal. If the pressure at the seal inlet is P, then Pr at radius r can be simplified as follows:

$$\mathrm{Pr}=P\frac{r-r_1}{r_2-r_1} \tag{15}$$

If the thrust F is greater than the internal friction force between the media, leakage will occur. The calculation formula of leakage is as follows:

$$Q=\frac{\pi Dh^3(p1-p2)}{12\mu L} \tag{16}$$

D is the inner diameter of the cylindrical surface formed by the seal. It can be seen from the above formula that the leakage of the ring seal is directly proportional to the third power of the sealing gap and the sealing pressure difference, and is inversely proportional to the sealing length. In theory, the smaller the backlash and the longer the length of the clearance seal, the better the sealing effect.

IV. Experimental Study

In this paper, a non-contact intermediate rotating ring mechanical seal structure is studied. The temperature field and thermal deformation of the seal ring are numerically simulated by COMSOL software. In this paper, the seal clearance of cylindrical ring with diameter of φ179.5mm, clearance of 0.5mm and axial seal length of 15mm is studied. The setting of boundary conditions is shown in Table 1. According to the definition of water conservancy diameter, the hydraulic diameter is the thickness of the gap, i.e. 0.5mm; As the gap seal is in a strong turbulence state, the turbulence density is set at 5%, the rotation center of the inner wall is at the eccentric position, and the rotation speed of the wall is the rotor speed.

TABLE I
Boundary Condition Setting

Parameter	Numerical Value
Inlet pressure	1.32MPa
Outlet pressure	0 MPa
Hydraulic diameter of inlet	0.5mm
Outlet hydraulic diameter	0.5mm
Turbulence density	5%
Outer wall	Stationary wall
Inner wall surface	Moving wall, the speed is the shaft speed

To present a better contrast of the traditional two ring (dynamic ring, static ring) non-contact mechanical seal and contact mechanical seal, and highlight the advantages of non-contact intermediate rotating ring mechanical seal, the three-dimensional model of two ring (moving ring, static ring) non-contact mechanical seal and contact mechanical seal are

established in this study. The structural form and geometric dimension of the sealing ring are shown in the figure, and the distributions of sealing pressure field and temperature field are shown in Figure 7.

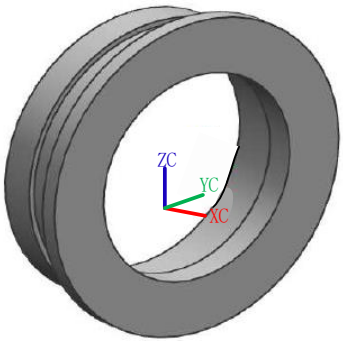

(a) Stationary ring

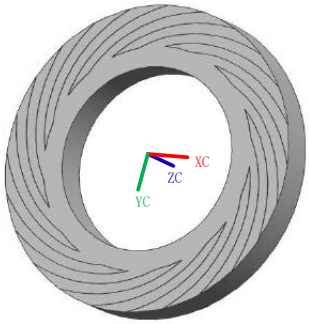

(b) Intermediate ring

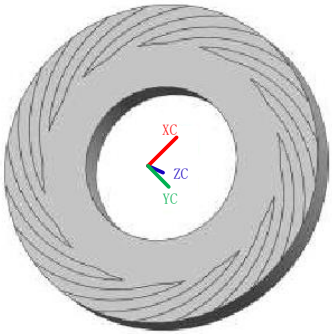

(c) Moving ring
Fig. 7. Structure of sealing ring

The mesh elements of triangle and tetrahedron can be divided by COMSOL mesh generator. Adaptive mesh generation can improve the quality of mesh automatically, and can also participate in the generation of mesh manually to achieve more accurate results. In this study, the mesh automatically generated by COMSOL can meet the requirements of solution, and the form of automatic mesh division by COMSOL is shown in Figure 8.

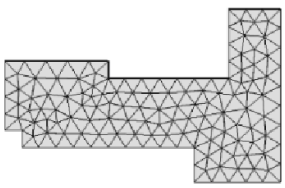

(a) Stationary ring

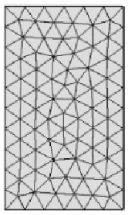

(b) Intermediate ring

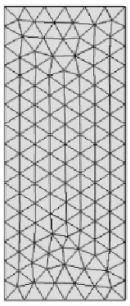

(c) Moving ring
Fig. 8. 2D mesh model of sealing ring

The dynamic mesh technique is used to simulate the flow field in the end face of mechanical seal, the distribution of wall shear stress f is obtained, and the friction torque is calculated:

$$D = 18 r_a \int_A f dA \tag{17}$$

Where r_a is the average radius of the sealing ring, and the arithmetic mean of the inner and outer diameters of the sealing ring is taken as $r_a = 27.5mm$. Masts-iv mechanical seal testing machine is adopted to test and collect the friction torque at different speeds. The friction torque values obtained by numerical simulation and test are shown in Table 1. T_1 is the common simulation friction torque, T_2 is the dynamic mesh simulation friction torque, T_3 is the test acquisition friction torque.

TABLE II
FRICTION TORQUE OBTAINED BY DIFFERENT METHODS

$n/(r\cdot\min^{-1})$	$T_1/(N\cdot m)$	$T_2/(N\cdot m)$	$T_3/(N\cdot m)$
2251	0.0334	0.0265	0.0210
2900	0.0424	0.0307	0.0310
3500	0.0505	0.0348	0.0415

It can be seen from Table 2 that the numerical simulation values obtained by using the dynamic mesh method are closer to the experimentally measured values at three different speeds, indicating that the dynamic grid method can obtain more realistic simulation results. The main reason is that the performance of gap seal is studied by computational fluid dynamics (CFD), and the effects of pressure difference, axial seal length and rotor speed on the performance of gap seal are analyzed.

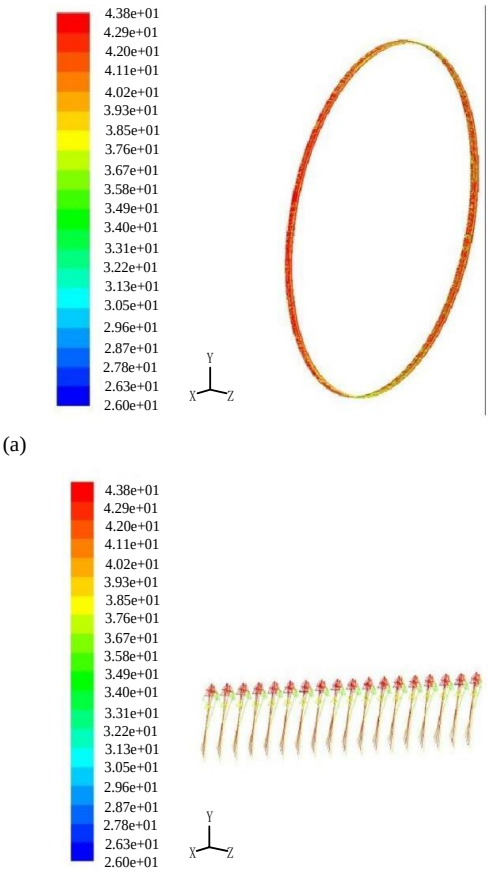

Fig. 9. The vector diagram of outlet velocity of conical ring seal and its local enlarged drawing

It can be seen from Figure 9 that the velocity difference at the inlet is very small, and there is almost no tangential velocity component, which shows little difference compared with the cylindrical mouth ring seal. The velocity at the outlet is obviously greater than that at the inlet, and there is a large tangential velocity component. The tangential velocity component of the conical ring seal is more obvious than that of the cylindrical ring seal. The main reason is that the dynamic layer updating method is used to update the dynamic grid, and the constant scale method is used to segment the grid.

By fixing the outlet pressure, the inlet pressure changes from 0.05Mpa to 2.5MPa. The relationship between leakage and pressure difference of cylindrical ring seal gap is obtained as shown in Figure 10.

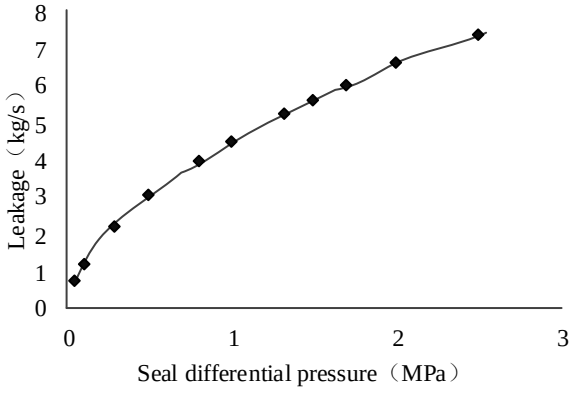

Fig. 10. Variation of leakage with pressure difference

It can be seen from Figure 10 that the leakage of seal gap increases with the increase of pressure difference, which is consistent with the theoretical calculation of leakage. The main reason is that this method uses computational fluid dynamics (CFD) to study the performance of clearance seals, and analyzes the influence of pressure difference, axial seal length and rotor speed on the performance of clearance seals.

The seal clearance leakage is calculated under the conditions of 310rad/s, 400rad/s, 500rad/s, 600rad/s and 700rad/s respectively, and the change curve of seal clearance leakage with rotating speed is obtained, as shown in Figure 11.

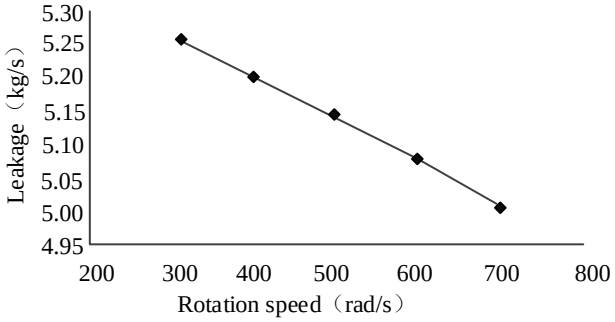

Fig. 11. Variation curve of leakage rate with rotating speed

The leakage rate varies linearly with the rotating speed, and the leakage rate is inversely proportional to the rotating speed. The greater the speed, the smaller the leakage of the seal.

Considering the influence of axial seal length on sealing performance, the seal gaps with axial seal lengths of 9mm, 10mm, 11mm, 12mm, 13mm and 15mm are considered in the research of this paper. The relationship between the leakage of the ring gap and the axial seal length is calculated, as shown in Figure 12.

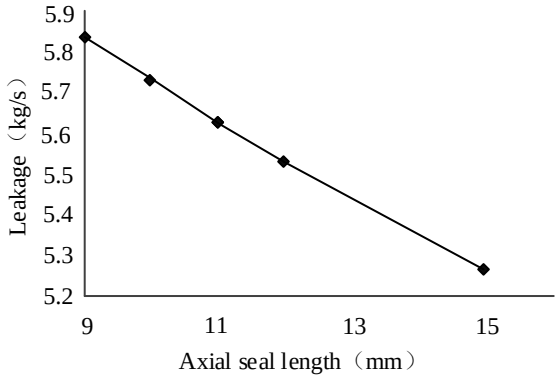

Fig. 12. Variation curve of leakage with axial seal length

Under the same diameter and seal gap, the longer the axial length of the seal, the smaller the leakage of the seal gap, and the leakage amount changes linearly with the axial seal length. The main reason is that dynamic grid technology is applied to the numerical simulation of the internal flow field of mechanical seals. In order to solve the problem of unpredictable liquid film thickness in the simulation process, more real internal flow field characteristics can be obtained.

In order to further verify the performance of non-contact mechanical seal and ignore the static pressure effect, it is assumed that the pressure outside the seal is also the environmental pressure, and the liquid film thickness and film pressure distribution are taken as the test indicators. The test results are shown in Figure 13. The results show that due to

the influence of roughness, the three-dimensional curve distribution of lubricant film and film pressure seems to ripple, which fully reflects the influence of surface morphology on the film pressure distribution of lubricant film.

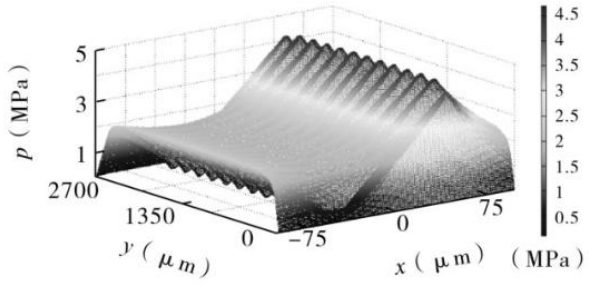

(a) Film thickness distribution

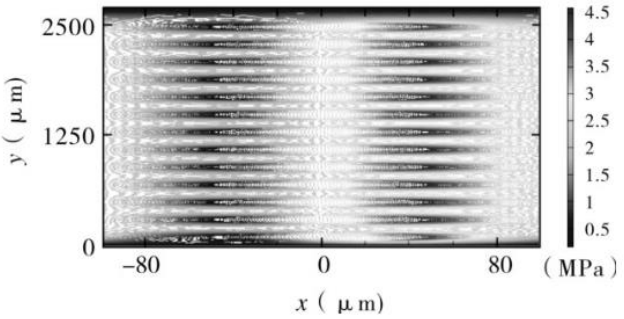

(b) Membrane pressure distribution

Fig. 13. Film thickness and pressure distribution of lubricating fluid in mechanical seals

V. Conclusion

The leakage of sealing clearance increases with the increase of pressure difference, changes linearly with the speed, but is inversely proportional to the speed. The greater the speed is, the smaller the leakage is. The longer the axial length of the seal is, the smaller the leakage is. It is feasible to apply dynamic mesh technology to the numerical simulation of internal flow field of mechanical seal. Compared with the existing simulation methods, the application of dynamic mesh technology can effectively obtain actual film thickness in seal operation, and can obtain simulation results closer to the real situation. There are many factors affecting the performance of mechanical seal, such as viscosity and temperature of fluid. However, the accuracy of CFD calculation for non-contact seal needs to be further discussed.

Reference

[1] T. Xu, H. Zhu, G. Feng, et al., "Numerical simulation of calcite vein formation and its impact on caprock sealing efficiency – Case study of a natural CO2 reservoir," *International Journal of Greenhouse Gas Control*, vol. 83, pp. 29-42, 2019.

[2] D. Wang, X. Yu, "Numerical simulation of erosion of valve sealing surface by high speed water flow based on ALE Method," *Journal of Physics: Conference Series*, vol. 1300, pp. 012006, 2019.

[3] L. Q. Wang, Z. L. Wei, S. M. Yao, et al., "Sealing performance and optimization of a subsea pipeline mechanical connector," *Chinese Journal of Mechanical Engineering*, vol. 31, no. 1, pp. 133-146, 2018.

[4] S. Mattana, M. Mattarelli, L. Urbanelli, et al., "Non-contact mechanical and chemical analysis of single living cells by microspectroscopic techniques," *Applied Science: Light Science*, vol, 7, no. 1, pp. 115-123, 2018.

[5] S. Mattana, M. Mattarelli, L. Urbanelli, et al., "Non-contact mechanical and chemical analysis of single living cells by microspectroscopic techniques," *Light, Ence Applications*, vol. 7, 2018.

[6] S. Y. Kong, X. Yang, Z. Y. Lee, "Mechanical performance and numerical simulation of GFRP-concrete composite panel with circular hollow connectors and epoxy adhesion," *Construction and Building Materials*, vol. 184, no. 30, pp. 643-654, 2018.

[7] V. Nekhaev, V. Nikolaev, M. Safronova, et al., "Numerical simulation of oscillations of a nonlinear mechanical system with a spring- loaded viscous friction damper," *MATEC Web of Conferences*, pp. 265, 2019.

[8] T. M. Rodgers, J. E. Bishop, J. D. Madison, "Direct numerical simulation of mechanical response in synthetic additively manufactured microstructures," *Modelling & Simulation in Materials Ence& Engineering*, vol. 26, no. 5, pp. 055010, 2018.

[9] M. Alizadeh, B. Nikkhahi, A. S. Farahani, et al., "Numerical study on the effect of geometrical parameters on the labyrinth-honeycomb seal performance," *Proceedings of the Institution of Mechanical Engineers*, vol. 232, no. 2, pp. 362-373, 2018.

[10] Y. Zhang, Y. Chen, D. Li, et al., "Experimental validation and numerical simulation of static pressure in multi-stage ferrofluid seals," *IEEE Transactions on Magnetics*, vol. 55, no. 3, pp. 1-8, 2019.

[11] B. Q. Wang, X. D. Peng, X. K. Meng, "Simulation of the effects of non-Newtonian fluid on the behavior of a step hydraulic rod seal based on a power law fluid model," *Journal of Zhejiang University - Science A: Applied Physics & Engineering*, vol. 19, no. 11, pp.824-842, 2018.

[12] J. Jiang, X. Zheng, S. Wu, et al., "Nondestructive experimental characterization and numerical simulation on self-healing and chloride ion transport in cracked ultra-high performance concrete," *Construction and Building Materials*, vol. 198, no. 20, pp. 696-709, 2019.

[13] S. Gao, G. Zhu, Y. Gao, et al., "Numerical simulation on thermodynamics performance in the fireproof sealing by finite element analysis," *Mathematical Problems in Engineering*, vol. 2019, no. 7, pp. 1-9, 2019.

[14] S. Tsala, Y. Berthier, G. Mollon, et al., "Numerical analysis of the contact pressure in a quasi-static elastomeric reciprocating sealing system," *Journal of Tribology*, vol. 140, no. 6, pp. 064502, 2018.

[15] Z. Chen, Z. Sun, B. Panicaud, "Constitutive modeling of TWIP/TRIP steels and numerical simulation of single impact during Surface Mechanical Attrition Treatment," *Mechanics of Materials*, vol. 122, pp. 69-75, 2018.

[16] R. Xiong, "Numerical simulation analysis of non-contact mechanical seal performance based on neural network," *2020 IEEE International Conference on Industrial Application of Artificial Intelligence (IAAI) IEEE*, 2020.

[17] L. Chen, Y. Zhang, Y. Cui, B. Zhi, J. Wang, M. Wang, "Numerical investigation on sealing performance of non-contact finger seal with herringbone groove surface topography," *Surface Topography: Metrology and Properties*, vol. 9, no. 4, pp. 045041, 2021.